

The statistical mechanics of inhomogeneous hard rod mixtures

T. K. Vanderlick^{a)} and H. T. Davis

Chemical Engineering and Materials Science, University of Minnesota, Minneapolis, Minnesota 55455

J. K. Percus

Courant Institute of Mathematics Sciences and Physics Department, New York University, New York, New York 10012

(Received 11 May 1989; accepted 8 August 1989)

The exact statistical mechanical solution to the problem of an equilibrium inhomogeneous classical one-dimensional mixture of hard rods is presented. From the solution, thermodynamic properties, density profiles, and correlation functions of hard rod fluids confined to small regions (micropores) can be calculated. The theory is applied to investigate microstructure, pore pressures, and pore adsorption selectivity of micropores in equilibrium with binary hard rod mixtures. A prescription is suggested for generalizing the one-dimensional results to higher dimensions.

I. INTRODUCTION

Fluids confined to small regions have microscopic structure and thermodynamics that are sensitive functions of the interaction between fluid and substrate. A number of models have been used, with some degree of success as judged by comparison with computer simulations, to represent the spectrum of behavior. One approach, with obvious attendant advantage, is to solve a special system exactly and extrapolate to realistic situations. The exact solvable models that are available are few and far between. Nonetheless, the inhomogeneous classical one-dimensional hard core fluid, for example, has sufficiently nontrivial structure that its implications for real systems are relatively easy to estimate. The solvability is in inverse form, i.e., external potential, or free energy, as functionals of density profile, but the simplicity of the results is striking.

In this paper, we extend the results previously obtained for one-component hard rod fluids to mixtures of fluids in restricted domains.^{1,2} The phenomenology is of course much more extensive, as is the nature of the input information. However, in conformity with the empirical success of simple scaling in representing the self-interaction of homologous molecular species, and of simple combining rules for representing their mutual interaction, it makes sense to regard a mixture of hard core fluids of different core diameters, and additive mutual cores, as a reasonable prototype to which extrapolation methods may be applied. The present work, then, consists of three parts. First, we carry out the reasonably straightforward extension of the nonuniform hard core fluid in one dimension to that of several interacting species. We then solve the resulting inverse relations to obtain density profiles for several components in constrained geometries, to get a feeling for the phenomenology as well as to model special physical situations. Finally, we indicate in sketchy fashion how extrapolation to real fluids might be made, but leave the matter of more complex computations to future work.

II. THE MODEL AND ITS SOLUTION

There are numerous physical cases in which fluids are confined to narrow channels. If these are narrow enough that two molecules cannot pass each other, then the molecules are ordered in a one-dimensional fashion, and if they are still narrower, the molecules are fully specified by their longitudinal positions (and parity if not symmetric). We may regard the limiting case of perfectly hard molecules as the one under consideration, but we hope it will serve as well as a prototype for extrapolation to softer interactions and three-dimensional geometry. For this purpose, the absence of strict ordering implies that we must consider an ensemble in which numbers of molecules of a given species are restricted—most conveniently by chemical potential—but in which they can reside in any order.

We will imagine that species α is acted upon by the external potential $u_\alpha(x)$ as well as the chemical potential μ_α in a grand ensemble. Only the combination

$$w_\alpha(x) = e^{\beta(\mu_\alpha - u_\alpha(x))} \quad (2.1)$$

appears in the grand potential Ξ_T , which, if the internal interaction Boltzmann factor is given by the step function

$$e_{\alpha\beta}(x, y) = \eta(x - y - a_{\alpha\beta}) \quad (2.2)$$

for mutual hard cores with type α -type β exclusion length $a_{\alpha\beta}$, can be written in condensed form as

$$\Xi_T = 1 + \langle 1 | w(I - ew)^{-1} | 1 \rangle. \quad (2.3)$$

Here, $e_{\alpha\beta}(x, y)$ is abbreviated as the matrix e on the space (x, α) of position and species, w refers to the diagonal matrix

$$w_{\alpha\beta}(x, y) = w_\alpha(x) \delta_{\alpha\beta} \delta(x - y), \quad (2.4)$$

1 to the vector

$$1_\alpha(x) = 1, \quad (2.5)$$

and the one-sided nature of (2.2) is responsible for the absence of $1/N!$ in the N -particle term of the expansion of (2.3).

The α -species density is now obtainable by functional differentiation:

^{a)} Present address: Department of Chemical Engineering, University of Pennsylvania, Philadelphia, Pennsylvania 19104-6393.

$$n_\alpha(x) = \frac{1}{\Xi_T} \frac{1}{\beta} \frac{\delta \Xi_T}{\delta [\mu_\alpha - u_\alpha(x)]}, \tag{2.6}$$

which works out to

$$n_\alpha(x) = (1/\Xi_T) \langle 1 | (I - ew)^{-1} | x \alpha \rangle \times w_\alpha(x) \langle x \alpha | (I - ew)^{-1} | 1 \rangle. \tag{2.7}$$

We may write (2.7) as

$$n_\alpha(x) = [w_\alpha(x)/\Xi_T] \hat{\Xi}_\alpha(x) \Xi_\alpha(x), \tag{2.8}$$

where the "truncated partition functions" satisfy

$$\Xi = 1 + ew\Xi, \tag{2.9}$$

$$\hat{\Xi} = 1 + \hat{\Xi}we; \tag{2.10}$$

here Ξ is regarded as a column vector and $\hat{\Xi}$ as a row vector. Our objective is to eliminate Ξ and $\hat{\Xi}$ from (2.8)–(2.10) in order to express $\mu_\alpha - u_\alpha$ as a function of n_α .

Ready solvability of (2.8)–(2.10) depends very much on the rank of the Fourier-transformed Boltzmann factor

$$\tilde{e}_{\alpha\beta}(k) = e^{ika_{\alpha\beta}/ik}. \tag{2.11}$$

The simplest case is that of additive exclusion lengths

$$a_{\alpha\beta} = \frac{1}{2}(a_\alpha + a_\beta), \tag{2.12}$$

in which case (2.11) is rank one, and we can write

$$e_{\alpha\beta} = e_\alpha \delta_\beta = \delta_\alpha e_\beta,$$

where

$$e_\alpha(x, y) = \eta(x - y - a_\alpha/2), \tag{2.13}$$

$$\delta_\alpha(x, y) = \delta(x - y - a_\alpha/2).$$

Now, e_α and δ_α are vectors in index space but operators in x space. Equations (2.9) and (2.10) then become

$$\Xi_\alpha = 1 + \sum_\beta e_\alpha \delta_\beta w_\beta \Xi_\beta, \tag{2.14}$$

$$\hat{\Xi}_\alpha = 1 + \sum_\beta \hat{\Xi}_\beta w_\beta \delta_\beta e_\alpha,$$

which we write as

$$\Xi_\alpha = 1 + e_\alpha \Lambda, \quad \Lambda = \sum_\beta \delta_\beta w_\beta \Xi_\beta, \tag{2.15}$$

$$\hat{\Xi}_\alpha = 1 + \hat{\Lambda} e_\alpha, \quad \hat{\Lambda} = \sum_\beta \hat{\Xi}_\beta w_\beta \delta_\beta;$$

all quantities are vectors or matrices on x space, the index dependence being spelled out explicitly.

It is convenient to start by eliminating w_β from Λ and $\hat{\Lambda}$, using (2.8):

$$\Lambda = \Xi_T \sum_\beta \frac{\delta_\beta n_\beta}{\hat{\Xi}_\beta}, \tag{2.16}$$

$$\hat{\Lambda} = \Xi_T \sum_\beta \frac{\delta_\beta n_\beta}{\Xi_\beta},$$

then eliminate Ξ_β and $\hat{\Xi}_\beta$ using (2.15),

$$\Lambda = \Xi_T \sum_\beta \frac{\delta_\beta n_\beta}{(1 + \hat{\Lambda} e_\beta)}, \tag{2.17}$$

$$\hat{\Lambda} = \Xi_T \sum_\beta \frac{\delta_\beta n_\beta}{(1 + e_\beta \Lambda)}.$$

Carrying out the spatial operations in (2.17), one has

$$\Lambda(x) = \frac{n_-(x)}{1 + \int_x^\infty \hat{\Lambda}(z) dz} \Xi_T, \tag{2.18}$$

$$\hat{\Lambda}(x) = \frac{n_+(x)}{1 + \int_{-\infty}^x \Lambda(z) dz} \Xi_T,$$

where

$$n_-(x) = \sum_\beta n_\beta \left(x - \frac{1}{2} a_\beta \right), \tag{2.19}$$

$$n_+(x) = \sum_\beta n_\beta \left(x + \frac{1}{2} a_\beta \right).$$

The index dependence has thus collapsed into two net densities, n_+ and n_- .

Now let us define

$$\Xi(x) = 1 + \int_{-\infty}^x \Lambda(z) dz, \tag{2.20}$$

$$\hat{\Xi}(x) = 1 + \int_x^\infty \hat{\Lambda}(z) dz,$$

so that (2.15) reads simply

$$\Xi_\alpha(x) = \Xi(x - \frac{1}{2} a_\alpha), \tag{2.21}$$

$$\hat{\Xi}_\alpha(x) = \hat{\Xi}(x + \frac{1}{2} a_\alpha).$$

According to (2.18) and (2.20),

$$\frac{d\Xi}{dx}(x) = \frac{n_-(x)}{\Xi(x)} \Xi_T, \tag{2.22}$$

$$\frac{d\hat{\Xi}}{dx}(x) = \frac{n_+(x)}{\Xi(x)} \Xi_T.$$

Hence $d[\Xi(x)\hat{\Xi}(x)]/dx = \Xi_T[n_-(x) - n_+(x)]$. But for a confined system, $n_\alpha(x)w_\alpha(x) \rightarrow 1$ as $x \rightarrow \infty$. From (2.8), then, $\Xi(x)\hat{\Xi}(x) \rightarrow \Xi_T$ as $x \rightarrow \infty$, and so

$$\Xi(x)\hat{\Xi}(x) = \Xi_T \left[1 + \int_{-\infty}^x [n_-(y) - n_+(y)] dy \right]. \tag{2.23}$$

Inserting (2.23) into (2.22), we obtain $d \ln \Xi(x)/dx = n_-(x)/[1 + \int_{-\infty}^x (n_-(y) - n_+(y)) dy]$, or since $\Xi(-\infty) = 1$,

$$\Xi(x) = \exp \int_{-\infty}^x \frac{n_-(y)}{1 + \int_{-\infty}^y [n_-(z) - n_+(z)] dz} dy. \tag{2.24}$$

Similarly, from $d \ln \hat{\Xi}(x)/dx = -n_+(x)/[1 + \int_{-\infty}^x (n_-(y) - n_+(y)) dy]$, we have

$$\hat{\Xi}(x) = \Xi_T \exp \int_{-\infty}^x \frac{-n_+(y)}{1 + \int_{-\infty}^y [n_-(z) - n_+(z)] dz} dy. \tag{2.25}$$

Substituting (2.24) and (2.25) into (2.8) via (2.21), we find the penultimate result

$$\beta(\mu_\alpha - u_\alpha(x)) = \ln n_\alpha(x) - \int_{-\infty}^{x-(1/2)a_\alpha} \frac{n_-(y)}{1 + \int_{-\infty}^y [n_-(z) - n_+(z)] dz} dy + \int_{-\infty}^{x+(1/2)a_\alpha} \frac{n_+(y)}{1 + \int_{-\infty}^y [n_-(z) - n_+(z)] dz} dy, \quad (2.26)$$

which is readily transformed into the local expression

$$\beta(\mu_\alpha - u_\alpha(x)) = \ln n_\alpha(x) - \frac{1}{2} \ln \left[1 - \sum_{\beta} \int_{x+\Delta_{\alpha\beta}}^{x+a_{\alpha\beta}} n_\beta(z) dz \right] - \frac{1}{2} \ln \left[1 - \sum_{\beta} \int_{x-a_{\alpha\beta}}^{x-\Delta_{\alpha\beta}} n_\beta(z) dz \right] + \int_{x-(1/2)a_\alpha}^{x+(1/2)a_\alpha} \frac{\sum_{\gamma} \frac{1}{2} [n_\gamma(y + \frac{1}{2}a_\gamma) + n_\gamma(y - \frac{1}{2}a_\gamma)]}{1 - \sum_{\beta} \int_{y-(1/2)a_\beta}^{y+(1/2)a_\beta} n_\beta(z) dz} dy, \quad (2.27)$$

where $a_{\alpha\beta} = \frac{1}{2}(a_\alpha + a_\beta)$ and $\Delta_{\alpha\beta} = \frac{1}{2}(a_\alpha - a_\beta)$.

Upon further transformation, Eq. (2.27) takes on the simpler local form

$$\beta[\mu_\alpha - u_\alpha(x)] = \ln \left[\frac{n_\alpha(x)}{1 - \sum_{\beta} \int_{x+\Delta_{\alpha\beta}}^{x+a_{\alpha\beta}} n_\beta(z) dz} \right] + \sum_{\gamma} \int_{x-a_{\alpha\gamma}}^{x+\Delta_{\alpha\gamma}} \frac{n_\gamma(y)}{1 - \sum_{\beta} \int_{y+\Delta_{\gamma\beta}}^{y+a_{\gamma\beta}} n_\beta(z) dz} dy. \quad (2.28)$$

A more concise summary is via the "internal" Helmholtz free energy

$$F^B = F - \int \sum_{\beta} n_\beta(z) u_\beta(z) dz, \quad (2.29)$$

which generates the profile equation according to

$$\mu_\alpha - u_\alpha(x) = \frac{\delta F^B}{\delta n_\alpha(x)}. \quad (2.30)$$

It is easily verified that (2.27) arises in this way from

$$\beta F^B(\{n\}) = \sum_{\alpha} \int [n_\alpha(x) \ln n_\alpha(x) - n_\alpha(x)] dx + \int \sum_{\alpha} \frac{1}{2} \left[n_\alpha \left(y + \frac{1}{2} a_\alpha \right) + n_\alpha \left(y - \frac{1}{2} a_\alpha \right) \right] \times \ln \left(1 - \sum_{\beta} \int_{y-(1/2)a_\beta}^{y+(1/2)a_\beta} n_\beta(z) dz \right) dy, \quad (2.31)$$

which is the simple expression we sought.

III. HARD RODS BETWEEN HARD WALLS

In the special case in which the external potential represents rigid walls

$$u_\alpha(x) = \infty, \quad x < a_\alpha/2, \quad x > L - a_\alpha/2, \\ = 0, \quad a_\alpha/2 < x < L - a_\alpha/2, \quad (3.1)$$

$$n^{(k)}(x_1, \dots, x_k) = \frac{\prod_{i=1}^k e^{\beta \mu_i} \Xi_T(x_1 - a_1/2) \prod_{l=2}^k \Xi_T[x_l - x_{l-1} - (a_l + a_{l-1})/2] \Xi_T(L - x_k - a_k/2)}{\Xi_T(L)}. \quad (3.6)$$

where L is the length of the system, the problem is greatly simplified. The canonical partition function can be solved analytically to obtain

$$Q_N = \prod_{\alpha} \frac{1}{N_{\alpha} \lambda_{\alpha}^{N_{\alpha}}} \eta \left(L - \sum_{\beta} N_{\beta} a_{\beta} \right) \left(L - \sum_{\beta} N_{\beta} a_{\beta} \right)^N, \quad (3.2)$$

where λ_{α} is the de Broglie wavelength, $\lambda_{\alpha} = (h^2 \beta / 2\pi m_{\alpha})^{1/2}$, and η is the step function. This result in turn yields for the grand canonical partition function

$$\Xi_T(L) = \sum_{\mathbf{N}} \prod_{\alpha} \frac{e^{\beta N_{\alpha} \mu_{\alpha}}}{N_{\alpha} \lambda_{\alpha}^{N_{\alpha}}} \eta \left(L - \sum_{\beta} N_{\beta} a_{\beta} \right) \times \left(L - \sum_{\beta} N_{\beta} a_{\beta} \right)^N, \quad (3.3)$$

where \mathbf{N} denotes the set N_1, \dots, N_c of occupation numbers of each component of the mixture.

The equilibrium value of any thermodynamic variable X in an open isothermal system can be computed from the grand canonical ensemble average of $X_{\mathbf{N}}$, the value of the variable in a canonical ensemble. Thus X can be computed from the expression

$$X = \sum_{\mathbf{N}} X_{\mathbf{N}} \mathcal{P}_{\mathbf{N}}, \quad (3.4)$$

in which the probability of a given occupancy \mathbf{N} is

$$\mathcal{P}_{\mathbf{N}} = \prod_{\alpha} e^{\beta N_{\alpha} \mu_{\alpha}} \frac{Q_{\mathbf{N}}}{\Xi_T(L)}. \quad (3.5)$$

Accordingly, the pressure P and mean density \bar{N}_i/L of component α can be calculated by substituting $P_{\mathbf{N}} = NkT/(L - \sum_{\beta} N_{\beta} a_{\beta})$ and N_{α}/L for $X_{\mathbf{N}}$ in Eq. (3.4).

Extending the derivation presented by Robledo and Rowlinson³ for the one-component case, we find for a mixture of hard rods the following k -body density distribution function:

In this equation $\Xi_T(y)$ denotes the grand potential for a system of length y . Thus the combination of Eq. (3.3), evaluated for L equal to the appropriate choices of y and Eq. (3.6) provides an analytic solution to the k -body density distribution function for a hard rod mixture confined between hard walls. In particular, the density of component α is given by

$$n_\alpha(x) = (e^{\beta\mu_\alpha}/\lambda_\alpha) \times [\Xi_T(x - a_\alpha/2)\Xi_T(L - x - a_\alpha/2)/\Xi_T(L)]. \quad (3.7)$$

IV. A NUMERICAL SURVEY

In this section we investigate the implications of the theory for the density profiles, selective adsorption, and pressure of binary mixtures confined between walls separated by a distance L . Given the wall potentials $u_\alpha(x)$, the density profiles $n_\alpha(x)$ can be obtained from the nonlinear system defined by Eq. (2.27). Alternatively, with the definition

$$h_\alpha(x) = \frac{n_\alpha(x)}{1 - \sum_\beta \int_{x-a_{\alpha\beta}}^{x+a_{\alpha\beta}} n_\beta(y) dy}, \quad (4.1)$$

Eq. (2.27) becomes

$$h_\alpha(x) = \exp\left\{\beta(\mu_\alpha - u_\alpha(x)) - \sum_\beta \int_{x-a_{\alpha\beta}}^{x+\Delta_{\beta\alpha}} h_\beta(y) dy\right\}. \quad (4.2)$$

To find the density profiles now, one has to solve the nonlinear system at Eq. (4.2) for h_α , insert this solution into Eq. (4.1), and solve the resulting linear equations for n_α . This procedure generates more work than does solving Eq. (2.27) directly. However, it has the advantage that for a one-component fluid it admits an analytic solution⁴ for the density profile and for a multicomponent fluid it yields a convergent solution by Picard iteration. The Picard iteration procedure is to guess a solution $h_\alpha^{(0)}$, insert it onto the right-hand side of Eq. (4.2), and compute a new estimate of $h_\alpha^{(1)}$. Next insert this estimation onto the right-hand side of Eq. (4.2) and generate the estimate $h_\alpha^{(2)}$. We continue this procedure to a k th step such that $\sum_\alpha \int |h_\alpha^{(k)}(x) - h_\alpha^{(k-1)}(x)| dx < \chi$, where χ is a small number compared to $\sum_\alpha \int h_\alpha^{(k)}(x) dx$. Typically we set χ equal to 10^{-4} .

In what follows we present a study of a binary mixture of hard rods confined to a one-dimensional "pore" whose fluid-wall potential is of the form

$$u_\alpha(x) = \infty, \quad x < a_\alpha/2, \quad x > L - a_\alpha/2, \\ = -\epsilon_\alpha \left\{ \left(\frac{a_\alpha}{x + a_\alpha/2} \right)^3 + \left(\frac{a_\alpha}{L + a_\alpha/2 - x} \right)^3 \right\}, \\ a_\alpha/2 < x < L - a_\alpha/2. \quad (4.3)$$

We consider two cases: (1) $\beta\epsilon_\alpha = 1$ and (2) $\epsilon_\alpha = 0$ and $\alpha = 1$ and 2. The second case is that of a hard rod mixture confined by hard walls and so the equations given in Sec. III can also be used to predict the desired quantities.

The pressure of the fluid in the pore can be computed from the formula

$$\beta P = \sum_\alpha n_\alpha \left(\frac{a_\alpha}{2} \right) - \sum_\alpha \frac{\beta}{2} \int_{a_\alpha/2}^{L-a_\alpha/2} n_\alpha(x) \frac{\partial u_\alpha}{\partial x}(x) dx. \quad (4.4)$$

When all $\epsilon_\alpha = 0$, the pressure can be computed from Eq. (4.4) or from Eq. (3.4) with $X_N = NkT/(L - \sum_\beta N_\beta a_\beta)$. The pressure of interest is the disjoining pressure Π , which is the difference between the pore pressure and the pressure P_b of a bulk phase in equilibrium with the pore fluid. Thus,

$$\Pi \equiv P - P_b. \quad (4.5)$$

The disjoining pressure can be measured in a surface force apparatus in which fluid is confined between mica sheets.^{5,6}

The relationship between the chemical potential and composition of the coexisting bulk phase is

$$\beta\mu_\alpha = \ln(\beta P_b x_\alpha^b) + \beta P_b a_\alpha, \quad (4.6)$$

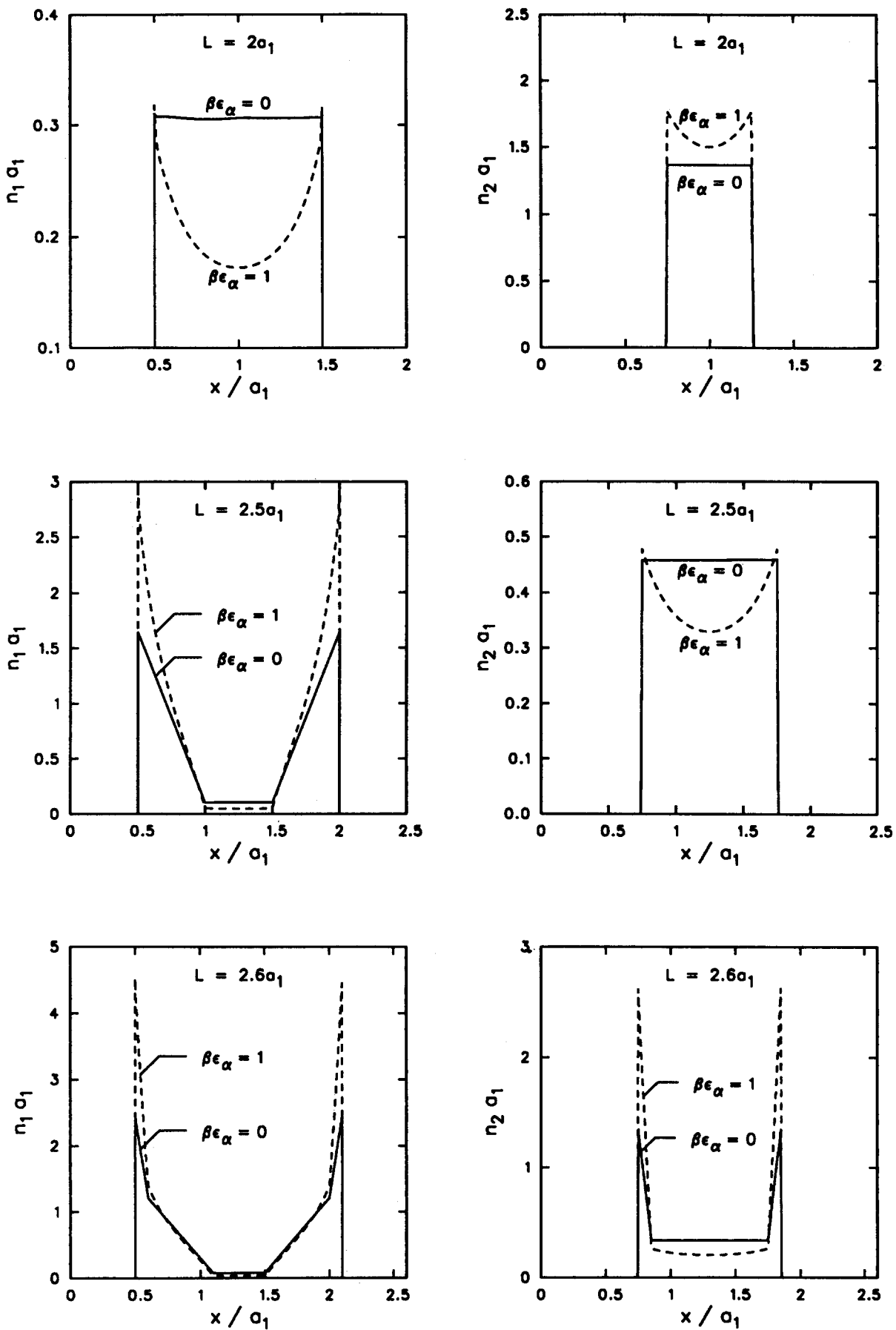
where x_α^b is the mole fraction of component α in bulk phase at pressure P_b and temperature T .

To simulate the conditions for a typical experiment in the surface force apparatus, we fix βP_b and mole fraction in bulk phase and then compute fluid properties as a function of pore width L . For all the computations reported in this section we used $\beta P_b a_1 = 3$.

Density profiles for hard walls ($\epsilon_\alpha = 0$) and walls with the attractive potential given by Eq. (4.3) ($\beta\epsilon_1 = \beta\epsilon_2 = 1$) are compared in Fig. 1. For these comparisons we chose $a_2 = 1.5a_1$ and $x_1^b = 0.5$. The profiles were determined from Eqs. (4.1) and (4.2) using the trapezoidal rule for integration and Picard iteration to solve the resulting nonlinear system.

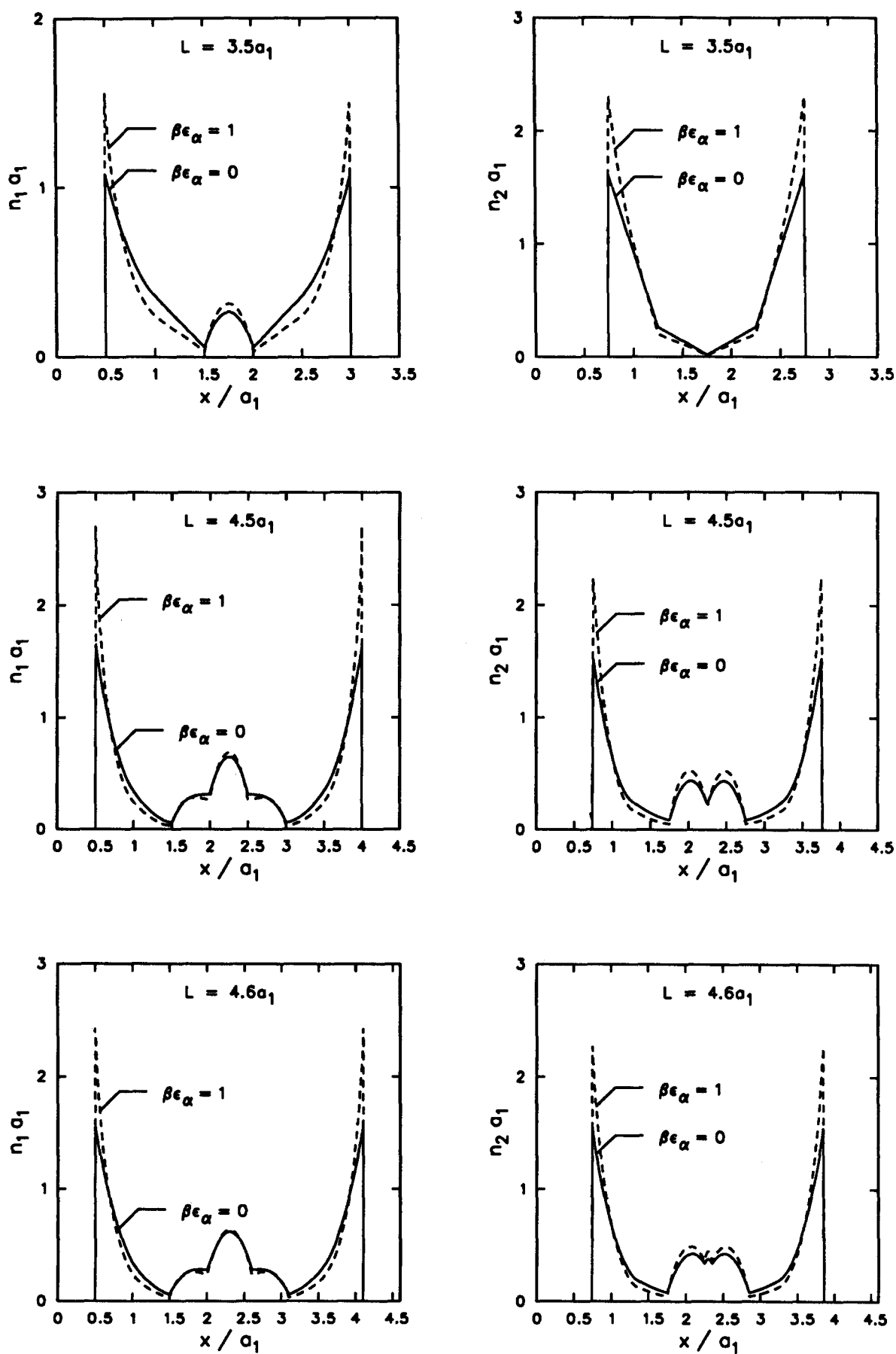
Unsurprisingly, the effect of wall attraction is to redistribute fluid in the pore in favor of higher densities at the pore walls. However, the packing constraints imposed by the hard rod repulsion is the dominant factor in controlling the qualitative structure of the density profiles. Consider first the hard wall case ($\epsilon_\alpha = 0$). For $L = 2a_1$, at most one particle of component 1 or 2 can occupy the pore. Thus the densities are uniform. For $L = 2.5a_1$, up to two particles of component 2 can occupy the pore, but component 2 can only occupy the pore if it is alone. Thus $n_1(x)$ has two peaks whereas n_2 is uniform. At $L = 2.6a_1$, both n_1 and n_2 have two peaks since two particles of component 1 or a particle of component 1 and one of component 2 can simultaneously occupy the pore. For $L = 3.5a_1$, $n_1(x)$ has three peaks, reflecting the possibility of pore occupancy of by as many as three particles of component 1. Note that $n_2(x)$ still has only two peaks, but the profile has kinks at $x = 1.25$ and 1.75 , which arise from triple pore occupancy: two particles of component 2 plus one of component 1. Similar consideration of allowed occupancy explains the profiles for the case $L = 4.5a_1$.

As illustrated by the plots in Fig. 1, the attractive wall interactions change the qualitative features of the density profiles relatively little, aside from increasing the density near the walls. The same is true of the disjoining pressure Π presented in Fig. 2. The oscillatory structure of Π arises from the same pore occupancy or packing statistics that dictate the trends observed in the density profiles. The effect of the



(a)

FIG. 1. Density profiles for binary hard rod mixtures confined between hard walls ($\epsilon_\alpha = 0$) and attractive walls ($\beta\epsilon_\alpha = 1$) for various pore widths L . Chemical potentials correspond to bulk phase pressure $P_b = 3kT/a_1$ and mole fraction $x_1^b = 0.5$.



(b)

FIG. 1. (Continued).

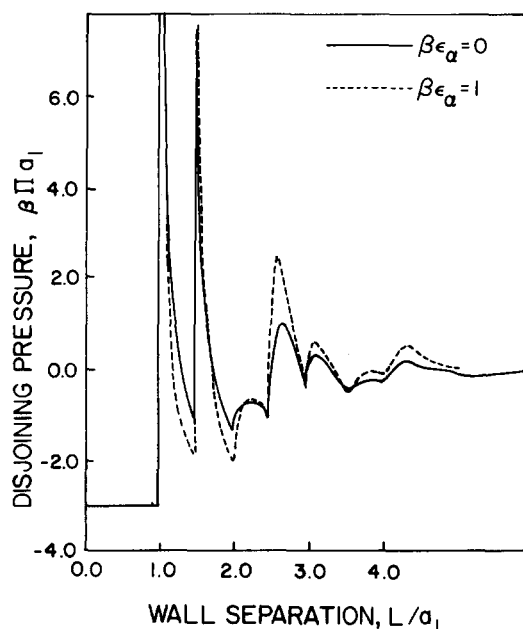


FIG. 2. Disjoining pressure, $\Pi \equiv P - P_b$, versus pore widths L . Coexisting bulk mixture has a bulk phase pressure $P_b = 3kT/a_1$ and mole fraction $x_1^b = 0.5$.

attractive walls is merely to exaggerate the maxima and minima that hard rod packing statistics cause in Π .

The selective adsorption of components of a fluid mixture in microporous media is of enormous technological importance. Zeolites, activated charcoal, silica gels, and diatomaceous earth represent significant examples of such media. The theory of hard rod mixtures can shed light on the effect of excluded volume (hard rod diameters in the one-dimensional case) on the selectivity. A measure of this selectivity is the pore average mole fraction of component 1, which is defined by

$$\bar{x}_1 = \frac{\int_0^L n_1(x) dx}{\int_0^L n_1(x) dx + \int_0^L n_2(x) dx}. \quad (4.7)$$

Since the bulk phase mole fraction is 0.5, a pore has adsorbed component 1 in preference to component 2 when $\bar{x}_1 > 0.5$ and it has adsorbed component 2 in preference to component 1 when $\bar{x}_1 < 0.5$. As illustrated in Fig. 3, pore selectivity is an oscillating function of the ratio of pore width to molecular diameter. Again, the major effect of wall attraction is to amplify the selectivity pattern dictated by the pore occupancy statistics of the hard rods.

Next we want to examine the dependence of the behavior of pore fluid on the composition of its coexisting bulk phase. The computation of density profiles, pore average densities, and pore pressures for hard rods confined by hard walls is considerably cheaper than for hard rods confined by attractive walls. This is because the formulas given in Sec. III can be employed to avoid having to solve integral equations. Since the qualitative behavior of confined hard rods is primarily controlled by the repulsive interactions in the dense fluid case considered here ($n_b a_1 = 0.75$), we have chosen for the more extensive calculations to examine dependence only for hard rods confined by hard walls. The composition study

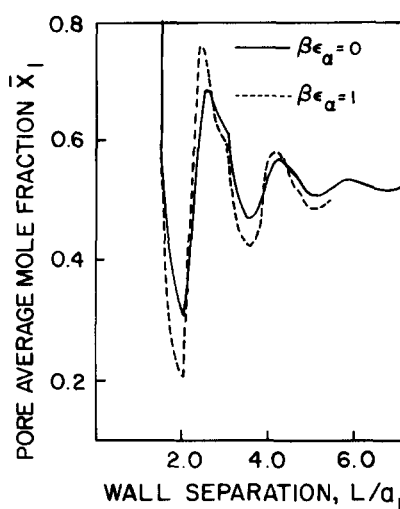


FIG. 3. Pore average mole fraction versus pore width. Same conditions as in Fig. 2.

was made for the mixture with $a_2 = 1.5a_1$ and $a_2 = 2.5a_1$ at a bulk pressure of $\beta P_b a_1 = 3$.

Density profiles are presented in Fig. 4 (results for the case $a_2 = 2.5a_1$ are shown only for $x_1^b = 0.5$ since they are qualitatively similar to those for $a_2 = 1.5a_1$). At pore widths large enough for several combinations of pore occupancy to occur (e.g., $L > 4a_1$ for the fluid with $a_2 = 1.5a_1$), the structure of the density profiles are quite sensitive to bulk composition x_1^b . Increasing x_1^b increases the chemical potential of component 1 relative to component 2 and, therefore, favors multiple pore occupancy by component 1. For example, for the separation $L = 5a_1$, when $x_1^b = 0.2$, triple occupancy by component 2 is favored at the expense of pore occupancy by component 1, whereas when $x_1^b = 0.8$ quadruple occupancy by component 1 is favored at the expense of pore occupancy by component 2. The result, illustrated by Figs. 5–8, is that pore selectivity and the disjoining pressure vary with pore separation L very differently at different bulk concentrations. Greater selectivity (as measured by \bar{x}_1/x_1^b) occurs at lower concentrations of component 1.

The behavior of the disjoining pressure of mixtures (Figs. 7 and 8) warrants special comment. The way the surface force apparatus is used presently, local maxima in the pressure will be observed only if the successive minima decrease in magnitude with increasing separation. Thus all the local minima and maxima predicted for a pure hard rod fluid would be observed by the current surface force apparatus technique. Mixtures, on the other hand, are predicted to have local maxima and minima that would not be observed. If this pattern of behavior carries over to three-dimensional fluids, it has important consequences for the interpretation of present data on mixtures and for the design of a new surface force apparatus.

V. EXTRAPOLATION TO HIGHER DIMENSIONS

The excess free energy, over that of an ideal gas mixture, takes the form for our model system

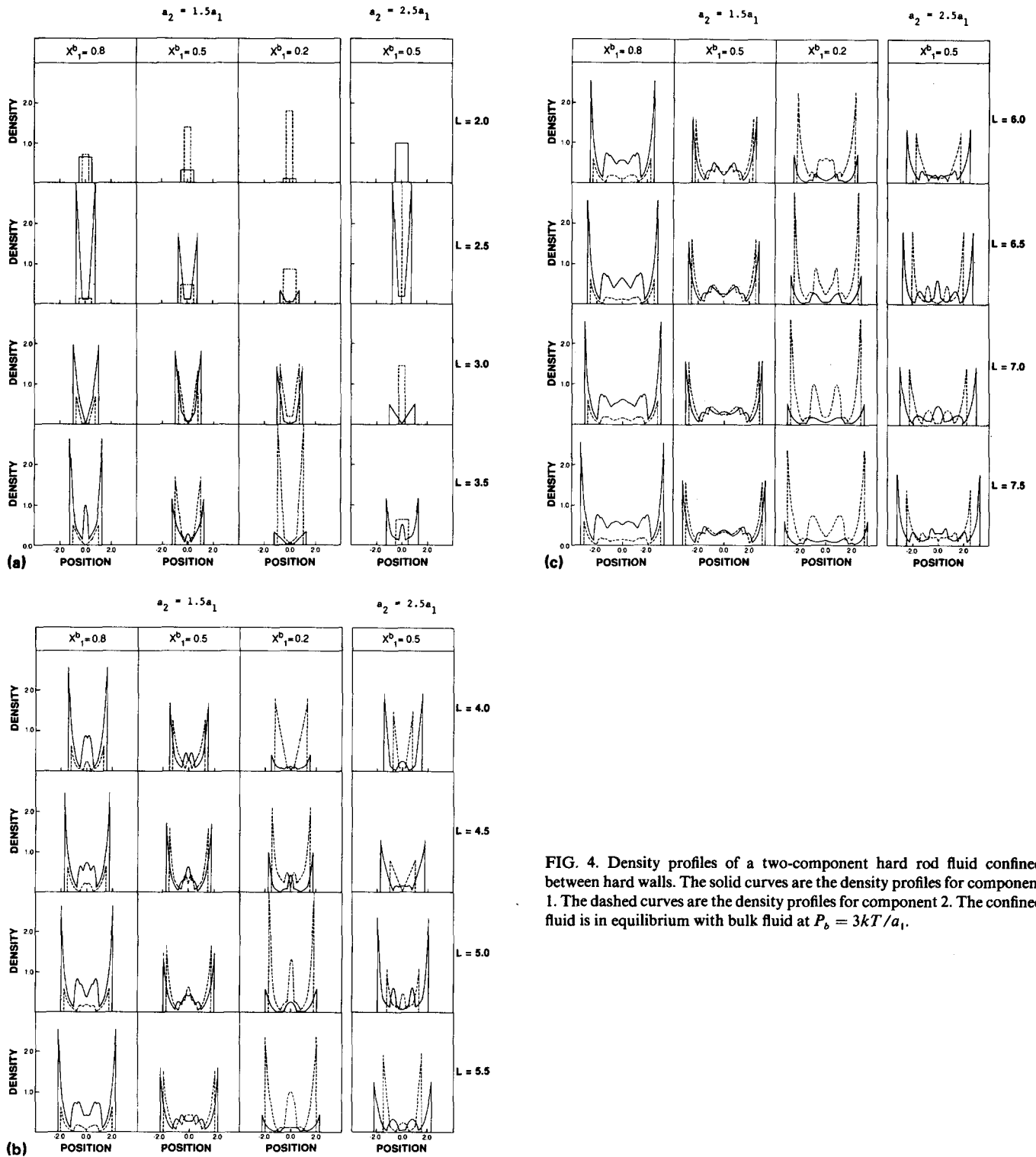


FIG. 4. Density profiles of a two-component hard rod fluid confined between hard walls. The solid curves are the density profiles for component 1. The dashed curves are the density profiles for component 2. The confined fluid is in equilibrium with bulk fluid at $P_b = 3kT/a_1$.

$$\begin{aligned}
 F^{ex}(\{n\}) = & -\frac{1}{\beta} \int \sum_{\alpha} \frac{1}{2} \\
 & \times \left[n_{\alpha} \left(y + \frac{1}{2} a_{\alpha} \right) + n_{\alpha} \left(y - \frac{1}{2} a_{\alpha} \right) \right] \\
 & \times \ln \left[1 - \sum_{\beta} \int_{y - (1/2)a_{\beta}}^{y + (1/2)a_{\beta}} n_{\beta}(z) dz \right] dy, \quad (5.1)
 \end{aligned}$$

which can be expressed more succinctly in terms of the total

surface-averaged density and volume-weighted density over the particle at the location in question:

$$\begin{aligned}
 \bar{n}_s(y) = & \sum_{\alpha} \frac{1}{2} \left[n_{\alpha} \left(y + \frac{1}{2} a_{\alpha} \right) + n_{\alpha} \left(y - \frac{1}{2} a_{\alpha} \right) \right], \\
 \bar{n}_v = & \frac{1}{a} \sum_{\beta} \int_{y + (1/2)a_{\beta}}^{y - (1/2)a_{\beta}} n_{\beta}(z) dz, \quad (5.2)
 \end{aligned}$$

where a is a reference diameter, as

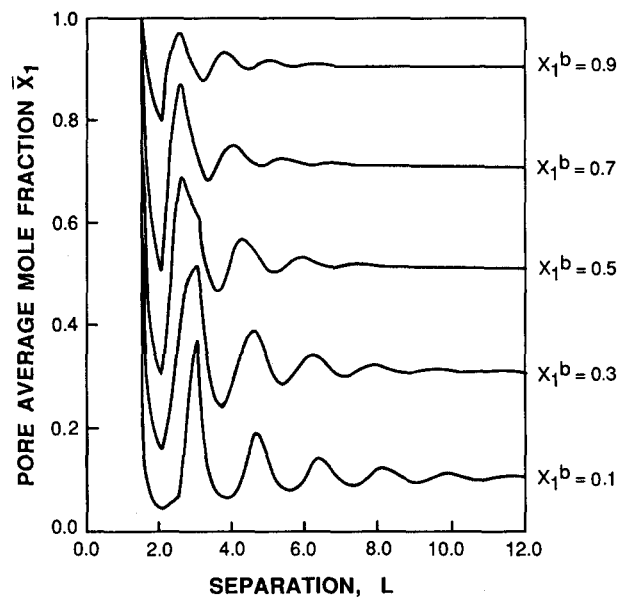


FIG. 5. Variation of pore average mole fraction with pore width in a binary fluid with $d_2 = 1.5d_1$. The bulk phase pressure is $P_b = 3kT/a_1$.

$$F^{\text{ex}}(\{\mathbf{n}\}) = -\frac{1}{\beta} \int \bar{n}_s(y) \ln(1 - a\bar{n}_v(y)) dy. \quad (5.3)$$

Since the corresponding specific (per particle) excess free energy for a uniform fluid is clearly

$$f^{\text{ex}}(\{\mathbf{n}\}) = -\frac{1}{\beta} \ln(1 - a\bar{n}_v), \quad \bar{n}_v = \sum \frac{a_\alpha}{a} n_\alpha, \quad (5.4)$$

model extensions to non-one-dimensional real mixtures are readily suggested.

A primitive example might be that of a mixture of three-dimensional hard cores, with exclusion diameters $a_{\alpha\beta}$

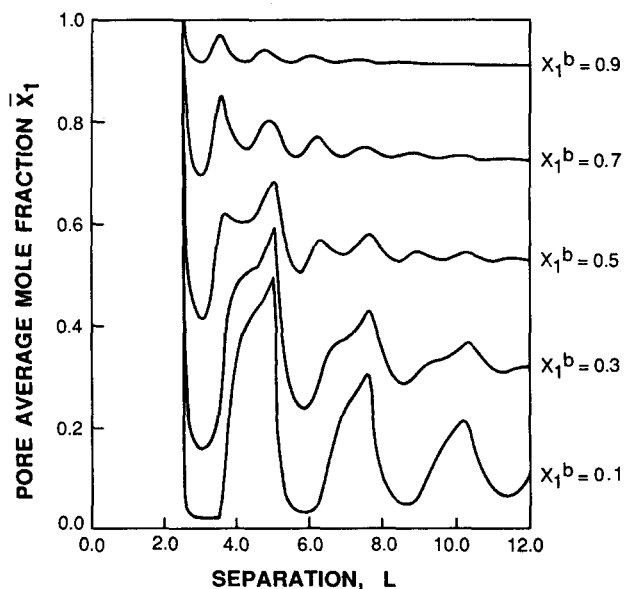


FIG. 6. Variation of pore average mole fraction with pore width in a binary fluid with $d_2 = 2.5d_1$. The bulk phase pressure is $P_b = 3kT/a_1$.

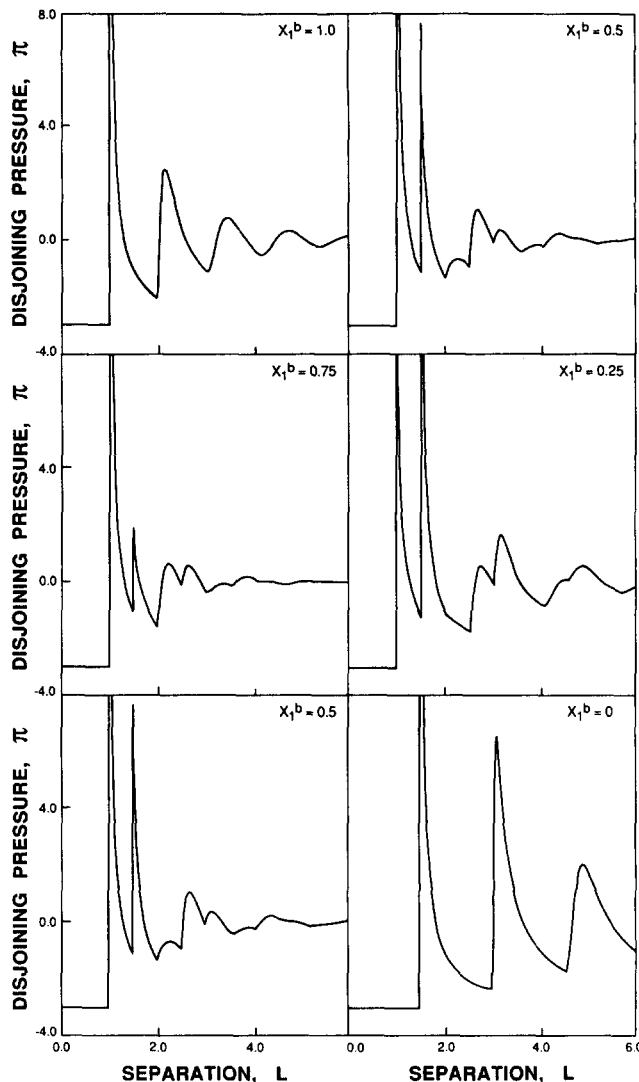


FIG. 7. Variation of disjoining pressure with pore width for a binary fluid with $d_2 = 1.5d_1$. The bulk phase pressure is $P_b = 3kT/a_1$.

$= \frac{1}{2}(a_\alpha + a_\beta)$, or exclusion volumes $v_{\alpha\beta} = 4\pi a_{\alpha\beta}^3/3$. A direct transcription of (5.2) and (5.3) would then be

$$F^{\text{ex}}(\{\mathbf{n}\}) = -\frac{1}{\beta} \int \bar{n}_s(\mathbf{r}) \ln(1 - v\bar{n}_v(\mathbf{r})) d^3\mathbf{r}, \quad (5.5)$$

where

$$\bar{n}_s(\mathbf{r}) = \frac{1}{4\pi} \int \sum_\alpha n_\alpha \left(\mathbf{r} + \frac{1}{2} a_\alpha \hat{\omega} \right) d^2\hat{\omega}, \quad (5.6)$$

$$\bar{n}_v(\mathbf{r}) = \frac{1}{v} \sum_\alpha \int_{|\mathbf{r}'| < a_\alpha} n_\alpha \left(\mathbf{r} + \frac{1}{2} \mathbf{r}' \right) d^3\mathbf{r}'. \quad (5.7)$$

Note that the uniform version

$$F^{\text{ex}} = -\frac{1}{\beta} \left(\sum_\gamma N_\gamma \right) \ln \left(1 - \sum v_\alpha n_\alpha \right) \quad (5.8)$$

is just the van der Waals excluded volume approximation, indeed the leading order of the more accurate Percus-Yevick (PY) approximation. More importantly, (5.5), as well as (5.1), mimic the one-component form, with the use of effective densities.

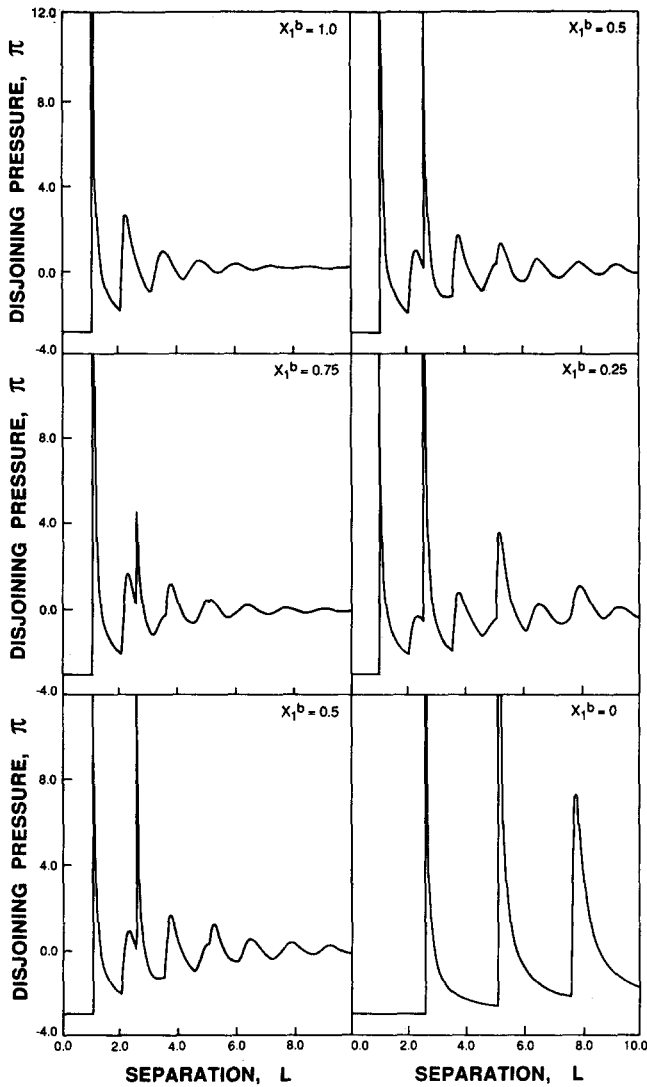


FIG. 8. Variation of disjoining pressure with pore width for a binary fluid with $d_2 = 2.5d_1$. The bulk phase pressure is $P_b = 3kT/a_1$.

Generalization to soft interacting mixtures is then also direct if, in the spirit of conformal mixture theory, we imagine that the thermodynamics is governed by the reference single-component specific free energy

$$f^{ex} = f^{ex} \left(\sum_{\gamma} \frac{v_{\gamma}}{v} n_{\gamma} \right), \tag{5.9}$$

where v is a volume associated with the reference particle, v_{γ} with the γ component. Then (4.3) would extend in model fashion to

$$F^{ex}(\bar{n}) = \int \bar{n}_s(\mathbf{r}) f^{ex}(\bar{n}_v(\mathbf{r})) d^3\mathbf{r}, \tag{5.10}$$

where

$$\bar{n}_s(\mathbf{r}) = \sum_{\alpha} \int n_{\alpha}(\mathbf{r} + \mathbf{r}') \sigma_{\alpha}(\mathbf{r}') d^3\mathbf{r}', \tag{5.11}$$

$$\int \sigma_{\alpha}(\mathbf{r}') d^3\mathbf{r}' = 1,$$

and

$$\bar{n}_v(\mathbf{r}) = \frac{1}{v} \sum_{\alpha} \int n_{\alpha}(\mathbf{r} + \mathbf{r}') \tau_{\alpha}(\mathbf{r}') d^3\mathbf{r}', \tag{5.12}$$

$$\int \tau_{\alpha}(\mathbf{r}') d^3\mathbf{r}' = v_{\alpha}.$$

Such a formulation might be expected to be appropriate when the interactions have the conformal structure

$$\phi_{\alpha\beta}(\mathbf{r}) = \frac{\epsilon_{\alpha\beta}}{\epsilon} \left(\frac{a}{a_{\alpha\beta}} \right)^3 \phi \left(\frac{a}{a_{\alpha\beta}} r \right) \tag{5.13}$$

in terms of a reference interaction with spatial scale a and reference energy ϵ . In this case, for $a_{\alpha\beta} = \frac{1}{2}(a_{\alpha} + a_{\beta})$, we would certainly want

$$v_{\alpha} = (\pi/6)a_{\alpha}^3, \quad v = (\pi/6)a^3, \tag{5.14}$$

but this still leaves the surface weights $\sigma_{\alpha}(\mathbf{r})$, volume weights $\tau_{\alpha}(\mathbf{r})$, and characteristic parameters ϵ and a to be determined. A number of options for the σ_{α} and τ_{α} have been discussed in the literature, as well as recipes for ϵ and a for a uniform system. Optimum resolution of these questions must be left for future work. Some preliminary three-dimensional studies have been reported in Ref. 6, where also are found more details of the numerical results given above.

ACKNOWLEDGMENTS

The authors wish to thank the National Science Foundation, the Department of Energy and the Minnesota Supercomputer Institute for partial support of this research. One of us (TKV) is grateful for an American Association of University Women's Dissertation Fellowship.

¹J. K. Percus, J. Stat. Phys. **15**, 505 (1976).
²J. K. Percus, J. Stat. Phys. **28**, 67 (1982).
³A. Robledo and J. S. Rowlinson, Mol. Phys. **58**, 711 (1986).
⁴T. K. Vanderlick, L. E. Scriven, and H. T. Davis, Phys. Rev. A **34**, 5130 (1986).
⁵H. K. Christenson, J. Chem. Phys. **78**, 6906 (1983); Chem. Phys. Lett. **118**, 455 (1985).
⁶T. K. Vanderlick, Ph.D. thesis, University of Minnesota, 1988.